

Spray dried microparticles for controlled delivery of mupirocin calcium: Process-tailored modulation of drug release

Marjana Dürriĝ¹, Ana Kwokal², Anita Hafner³, Maja Šegvić Klarić³, Aleksandra Dumić¹, Biserka Cetina-Čižmek¹ and Jelena Filipović-Grčić³

¹PLIVA Croatia Ltd., Research and Development, Prilaz baruna Filipovića 29, 10000 Zagreb, Croatia,

²PLIVA Croatia Ltd., TAPI Croatia, TAPI Research and Development, Prilaz baruna Filipovića 29, 10000 Zagreb, Croatia, and ³Faculty of Pharmacy and Biochemistry, Department of Pharmaceutical Technology, University of Zagreb, A. Kovačića 1, 10000 Zagreb, Croatia

Abstract

Spray dried microparticles containing mupirocin calcium were designed as acrylic matrix carriers with modulated drug release for efficient local drug delivery at minimum daily dose. Particle generation in spray drying and its effect on release performance were assessed by varying drug:polymer ratios with consequently altered initial saturations. Narrow-sized microparticles with mean diameters of 1.7–2.5 μm were obtained. Properties of the generated solid dispersions were examined by X-ray, thermal (thermo-gravimetric analysis, modulated differential scanning calorimetry) and spectroscopic (Fourier transformed infrared, Fourier transformed Raman) methods and correlated with drug loading and *in vitro* release. The best control over mupirocin release was achieved for 2:1 (w/w) drug:polymer ratio and found to be strongly process-dependent. For a particular ratio, increased feed concentration (>4%) boosted while increased inlet temperature (≥100°C) reduced drug release. Antimicrobial activity testing confirmed that encapsulated drug preserved its antibacterial effectiveness. Conclusively, spray drying was proven as a suitable method for preparing structured microparticles which can control drug release even at exceptionally high drug loadings.

Keywords: Mupirocin calcium, spray drying, solid dispersions, controlled release

Introduction

Mupirocin calcium (Figure 1) is a topical antibiotic agent chemically derived from pseudomonic acid that has a growth inhibiting effect, mainly against Gram-positive and some Gram-negative bacteria, by inhibiting bacterial protein synthesis due to its binding with isoleucyl transfer RNA synthetase (Ward and Campoli-Richards, 1986). It is primarily bacteriostatic at low concentrations, although it is usually bactericidal at high concentrations. It is presently used not only in various formulations for the treatment of secondarily infected traumatic skin lesions due to susceptible strains of *Staphylococcus aureus* and *Streptococcus pyogenes* but also as an intranasal topical agent for the

eradication of nasal colonisation with methicillin-resistant *S. aureus* (MRSA). It is used three times daily throughout therapy duration (up to 10 days). Multiple daily administrations often diminish patient acceptance and compliance, simultaneously jeopardising curing success. Therefore, a reasonable need exists to develop a drug delivery system that enables extended drug release for the improvement of mupirocin calcium therapy. Amrutiya et al. (2009) recently reported the development of mupirocin-loaded microsponges using an emulsion solvent diffusion method with ethylcellulose polymer.

Microparticles designed to control drug release into the skin ensure that the drug remains localised at the application site and does not unnecessarily enter into the

Address for correspondence: Jelena Filipović-Grčić, Faculty of Pharmacy and Biochemistry, Department of Pharmaceutical Technology, University of Zagreb, A. Kovačića 1, 10000 Zagreb, Croatia. Tel: +38516394761. Fax: +38514612691. E-mail: jfilipov@pharma.hr

(Received 16 May 2010; accepted 20 Oct 2010)
<http://www.informahealthcare.com/mnc>

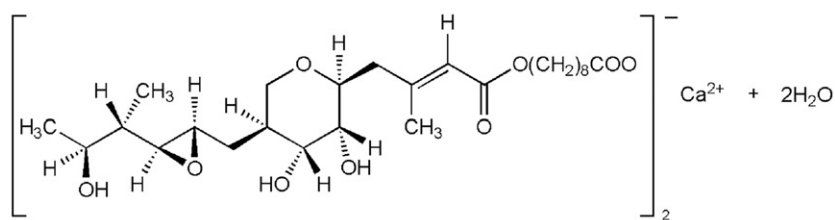


Figure 1. Mupirocin calcium dihydrate.

Source: Bactroban cream, Available at: http://us.gsk.com/products/assets/us_bactroban_cream.pdf. Accessed 10 November 2010.

systemic circulation (Embil and Nacht, 1996). They act as reservoirs releasing an active ingredient over an extended period of time maintaining effective drug concentration in the skin and, at the same time, reducing undesired side effects. Thus, periods of over-medication and under-medication are eliminated. This is especially important in the treatment of infectious diseases due to the prevention of antimicrobial resistance. Such delivery systems may also increase drug stability or improve incorporation into appropriate vehicles.

Certain articles describe the use of a spray drying technique for the preparation of controlled-release microparticles (Kristmundsdóttir et al., 1996; Pignatello et al., 1997; Esposito et al., 2000; Cortesi et al., 2007; Rattes and Oliveira, 2007; Al-Zoubi et al., 2008; Chen et al., 2008; Rassu et al., 2008) utilising water-insoluble and low-permeability acrylic polymers, e.g. ammonium methacrylate copolymers (Eudragit® RS). Specifically, Rattes and Oliveira (2007) have found that an increase in feed flow rate enlarged the mean particle diameter and obtained slower drug release. Esposito et al. (2000) and Rassu et al. (2008) reported that the increase in inlet temperature resulted in the reduction of microparticle size, while no correlation to drug release was reported. It was shown that the solvent type determines the structure of resultant microparticles influencing the drug release pattern (Kristmundsdóttir et al., 1996). The increase in the polymer-to-drug ratio resulted in decreased drug release (Al-Zoubi et al., 2008). Pignatello et al. (1997) have shown that, due to the high porosity of spray dried microparticles, drug release is poorly controlled.

Spray drying is a one-step, but complex, technological process that enables the adjustment of many parameters. In light of current reports on particle engineering approaches (Hadinoto et al., 2007; Vehring, 2008; Kawakami et al., 2010) understanding how the variation of parameters will affect the physicochemical properties of a product and its performance is considered essential. It is necessary to have full understanding of the physical state of the drug in microparticles, as these attributes may profoundly affect the release behaviour. However, it is also evident that no individual parameter, but rather a combination of all factors, is responsible for controlling the output.

The purpose of this study was to investigate spray drying encapsulation of mupirocin calcium into acrylic microparticles with the ultimate goal to modulate drug release for efficient local drug delivery at a minimum

daily dose. To the best of our knowledge, this is the first attempt to encapsulate mupirocin calcium into acrylic polymer microparticles by spray drying. Additionally, we aimed to assess particle generation in spray drying and its effect on release performance by varying different drug:polymer ratios, namely 5:1; 2:1; 1:1; 1:2 and 1:5 (w/w). The microparticles were evaluated with respect to encapsulation efficiency, production yield, particle size, morphology, *in vitro* drug release and solid-state properties.

Materials and methods

Materials

Mupirocin calcium was kindly donated by Pliva Croatia Ltd., Zagreb, Croatia. Eudragit® RS 100 (ammonio methacrylate copolymer type B, NF) was obtained from Evonik, Essen, Germany. Methanol and tetrahydrofuran of the grade intended for liquid chromatography and ammonium acetate p.a. were provided by Merck KgaA, Darmstadt, Germany. Sodium acetate trihydrate, p.a. was provided by Kemika, Zagreb, Croatia. Potassium bromide for infrared (IR) spectroscopy was obtained from Merck, Darmstadt, Germany. Ultrapure water was used in all experiments.

Preparation of microparticles

Drug-loaded microparticles were prepared by spray drying methanol solutions containing different ratios of Eudragit® RS 100 polymer and mupirocin calcium. Eudragit® RS 100 was dissolved in methanol using the ultrasonic bath until complete dissolution of polymer was achieved and left for 24 h before the drug was added. Mupirocin calcium has been dissolved in the polymer solution by gentle stirring and spray dried immediately. The following weight ratios (w/w) of drug and polymer were used: 5:1; 2:1; 1:1; 1:2 and 1:5. The total amount of solid material dissolved in the spraying solution (feed concentration) was 3% (w/w) for all experiments. In addition, the samples containing 2:1 (w/w) drug:polymer ratio having feed concentrations of 1%, 2%, 4% and 5% (w/w) were also prepared.

Spray drying was performed using a Büchi B-290 mini spray drier (Büchi Labortechnik AG, Flawil, Switzerland) with the Inert Loop B-295, which enabled safe operation

with organic solvents in a closed loop. The spray dryer operates by the co-current flow of a nitrogen (spraying medium) and product stream with an integrated two-fluid 0.7-mm nozzle. Compressed nitrogen was used to disperse the liquid into fine droplets, which were consequently dried in the cylinder and deposited in the cyclone. Drying conditions are given as follows for all prepared samples: the aspirator setting was 85%; the pump flow rate was 40% and the compressed nitrogen flow rate was 670 NL/h. A small high-performance cyclone was used to increase the yield. The inlet temperature was varied for different experiments; details are given in Tables 1–3. The drug was individually spray dried from 2% (w/w) methanol solutions under the same processing conditions as the corresponding microparticles at 100°C to obtain the amorphous drug. The spray dried polymer was produced in the same way. The amorphous materials of drug and polymer were used for comparison purposes. All obtained powders were collected in glass containers and stored in desiccators at the ambient temperature.

Determination of drug loading

Mupirocin calcium content in the microparticles was determined by the HPLC assay method described in the United States Pharmacopeia (USP), 31st edition, Suppl. 2, 2009. An appropriate amount of microparticles was dissolved in methanol under sonication in an ultrasonic bath (Julabo USR3, Julabo Labor Technik GmbH, Seelbach, Germany) for 30 min to obtain 0.1 mg/mL of mupirocin calcium. An HPLC system, which consisted of an Agilent 1100 Series instrument (Agilent Technologies, Waldbronn, Germany) equipped with a diode array detector set at 230 nm, was used to perform the assay. The mobile phase, a degassed and filtered mixture of 0.1 M ammonium acetate and tetrahydrofuran in the ratio of 68:32, was used at a flow rate of 1 mL/min. The column (Zorbax Eclipse XDB C8 column 250 × 4.6 mm², particle size 5 μm, Agilent, Palo Alto, CA, USA) suited with a guard column (Symmetry C8, particle size 5 μm, 3.9 × 20 mm, Waters, Dublin, Ireland) was operated at 35°C. The sample

Table 1. Characteristics of the microparticles spray dried at 100°C containing different drug:polymer ratios (w/w).

Sample (drug:polymer ratio, w/w)	Drug loading (% ± SD)	Mean spherical diameter (μm ± SD)	T_g (°C ± SD)	T_g' (°C ± SD)	GT (°C)	Residual solvent (% ± SD)
I (1:5)	15.7 ± 0.1	1.85 ± 1.40	60.7 ± 2.6	59.0 ± 0.4	~59.5	0.94 ± 0.01
II (1:2)	31.7 ± 0.2	2.25 ± 1.86	66.9 ± 1.3	78.8 ± 1.4	~62.4	0.80 ± 0.01
III (1:1)	47.6 ± 0.7	2.25 ± 1.86	66.7 ± 1.4	78.3 ± 0.1	~65.7	0.98 ± 0.03
IV (2:1)	63.7 ± 1.4	1.74 ± 1.29	65.5 ± 1.3	76.8 ± 0.4	~69.3	1.24 ± 0.05
V (5:1)	78.1 ± 2.8	2.45 ± 1.89	66.3 ± 0.8	77.3 ± 0.6	~73.3	1.32 ± 0.09

Notes: Drug loading - percent ratio (% w/w) of drug present in microparticles; SD - standard deviation ($n = 3$); T_g - glass transition temperature; T_g' - glass transition temperature after heat-cool-heat cycle and GT - Gordon-Taylor prediction of T_g value of drug and polymer mixture calculated using Equations (1) and (2).

Table 2. Characteristics of the microparticles containing drug:polymer ratio 2:1 (w/w) spray dried from 3% (w/w) feed solution at different inlet temperatures.

Sample	Inlet temperature (°C)	Outlet temperature (°C)	Drug loading (% ± SD)	Mean spherical diameter (μm ± SD)	T_g (°C ± SD)	Residual solvent (% ± SD)
IV-110	110°C	70–60°C	64.1 ± 0.3	1.88 ± 1.54	67.2 ± 1.9*	1.12 ± 0.09
IV-100	100°C	65–53°C	63.7 ± 1.4	1.74 ± 1.29	65.5 ± 1.3	1.24 ± 0.05
IV-90	90°C	56–46°C	63.6 ± 0.0	2.01 ± 1.55	62.9 ± 2.4	1.32 ± 0.03
IV-80	80°C	47–41°C	62.4 ± 0.1	2.49 ± 2.10	62.8 ± 2.4	1.33 ± 0.08
IV-70	70°C	41–37°C	63.5 ± 0.3	2.18 ± 1.96	59.7 ± 3.6*	1.44 ± 0.08

Table 3. Characteristics of the microparticles containing drug:polymer ratio 2:1 (w/w) spray dried at 100°C from different feed solutions.

Sample	Feed concentration (%; w/w)	Drug loading (% ± SD)	Mean spherical diameter (μm ± SD)	T_g (°C ± SD)	Residual solvent (% ± SD)
IV-1%	1	63.7 ± 0.0	2.02 ± 1.86	66.7 ± 1.1	1.14 ± 0.17
IV-2%	2	64.0 ± 0.3	1.72 ± 1.40	65.5 ± 2.5	1.17 ± 0.15
IV-3%	3	63.7 ± 1.4	1.74 ± 1.29	65.5 ± 1.3	1.24 ± 0.05
IV-4%	4	63.9 ± 0.5	2.46 ± 1.83	65.7 ± 2.1	1.08 ± 0.17
IV-5%	5	63.7 ± 0.5	2.67 ± 1.87	63.1 ± 1.5	1.57 ± 0.06

Notes: Drug loading - percent ratio (% w/w) of drug present in microparticles; SD - standard deviation ($n = 3$) and T_g - glass transition temperature.

injection volume was 20 μ L. The elution was isocratic and the run time was 10 min. All experiments were performed in triplicate, and the mean of the obtained values has been reported. Drug loading was determined as a percent ratio (w/w%) of the drug present in the microparticles.

In vitro drug release study

Drug release study was performed using a USP Apparatus 2 paddle apparatus (PharmaTest type PTW S, PharmaTest Apparatebau GmbH, Hainburg, Germany). A predetermined amount of microparticles was placed into 500 mL of degassed pH 5.5 USP acetate buffer, and the temperature was maintained at $37 \pm 0.5^\circ\text{C}$. The paddle speed was 20 rpm. Aliquots (5 mL) were withdrawn at predetermined time points, filtered through glass fibre prefilters (Acrodisc[®] GF 25-mm syringe filters with GF/0.45 GHP membrane, Pall, Bad Kreuznach, Germany) and analysed, according to the HPLC assay method described above. The withdrawn aliquots were replaced with fresh dissolution medium thermostated at 37°C . The amount of microparticles was calculated to maintain the sink condition of mupirocin calcium in the given medium pH (the solubility of mupirocin calcium amorphous in pH = 5.5 acetate buffer is more than 20 mg/mL). The targeted drug concentration was 0.1 mg/mL if complete release from microparticles is assumed. All analyses were performed in triplicate.

Mupirocin release kinetics were modelled using mono-exponential and biexponential equations (Table 4; GraphPad Prism, GraphPad Software Inc., San Diego, CA, USA; www.graphpad.com) to better understand the release behaviour of the microparticles. A biexponential model has been used to separate burst (k_1 rate constant) and sustained release phases (k_2 rate constant) of dissolution profiles and enable their comparison (Beck et al., 2007; Lionzo et al., 2007).

Particle size analysis

A microscopic image analysis technique for the determination of microparticle size distribution was applied. The particle size distributions (based on the numbers of particles) were determined using an Olympus BH-2 microscope equipped with a camera (CCD Camera ICD-42E; Ikegami Tsushinki Co., Tokyo, Japan) and computer-controlled image analysis system (Optomax V, Cambridge, UK). The microspheres were dispersed on a microscope slide. A microscopic field was scanned by video camera. The images of the scanned fields were digitised and analysed by the software (Optomax V Software, Cambridge, UK). In all measurements, at least 3000 particles were examined.

Thermal analyses

Modulated differential scanning calorimetry (MDSC) analyses were carried out in a TA Instrument modulated DSC Q1000 (TA Instruments, New Castle, DE, USA) using aluminium hermetic pans with pierced lids (to allow removal of residual solvent) with about 2–4 mg of sample, under dynamic nitrogen atmosphere (50 mL/min). The samples were heated at $5^\circ\text{C}/\text{min}$ from 20°C to 200°C using a modulation of $\pm 0.8^\circ\text{C}$ (amplitude) each 60 s (period). The glass transition temperature (T_g) was determined using the TA universal analyses software by extrapolating the linear portion of the DSC curve above and below the glass transition point and determining the midpoint temperature in the reverse heat flow curve. The analyses were done in triplicate.

Additionally, the samples were subjected to a cyclic heating programme (heat-cool-heat). The programme included sample heating up to 200°C and cooling back to 20°C under controlled conditions (ramp $5^\circ\text{C}/\text{min}$) following a second heating run from 20°C up to 200°C at $5^\circ\text{C}/\text{min}$.

Table 4. Model parameters of mupirocin calcium release from Eudragit[®] RS spray dried microparticles.

Sample	Monoexponential model $Q = 100(1 - e^{-kt})$		Biexponential model $Q = 100[1 - (Ae^{-k_1t} + Be^{-k_2t})]$				
	R^2	k_1 (min^{-1})	R^2	A	k_1 (min^{-1})	B	k_2 (min^{-1})
I	0.9765	0.265 ± 0.033	0.9999	0.635 ± 0.017	0.479 ± 0.044	0.220 ± 0.025	0.028 ± 0.004
II	0.9901	0.337 ± 0.030	0.9999	0.761 ± 0.018	0.521 ± 0.045	0.161 ± 0.025	0.033 ± 0.005
III	0.9900	0.293 ± 0.024	0.9976	0.642 ± 0.119	0.556 ± 0.229	0.232 ± 0.130	0.064 ± 0.024
IV*	0.9434	0.134 ± 0.028	0.9944	0.506 ± 0.036	0.376 ± 0.063	0.356 ± 0.053	0.025 ± 0.005
V	0.9922	0.349 ± 0.019	0.9999	0.792 ± 0.007	0.503 ± 0.016	0.142 ± 0.010	0.030 ± 0.002
IV-110	0.9624	0.047 ± 0.011	0.9996	0.321 ± 0.029	0.346 ± 0.061	0.555 ± 0.042	0.024 ± 0.002
IV-90	0.9838	0.362 ± 0.070	1.0000	0.761 ± 0.005	0.599 ± 0.031	0.176 ± 0.010	0.021 ± 0.002
IV-80	0.9886	0.324 ± 0.049	0.9999	0.786 ± 0.010	0.483 ± 0.025	0.168 ± 0.016	0.027 ± 0.003
IV-70	0.9846	0.305 ± 0.051	0.9999	0.724 ± 0.007	0.466 ± 0.018	0.177 ± 0.011	0.024 ± 0.002
IV-5%	0.9894	0.271 ± 0.036	0.9999	0.759 ± 0.010	0.424 ± 0.017	0.168 ± 0.015	0.027 ± 0.003
IV-4%	0.9305	0.112 ± 0.037	1.0000	0.492 ± 0.002	0.315 ± 0.006	0.372 ± 0.007	0.015 ± 0.000
IV-2%	0.9994	0.090 ± 0.026	0.9997	0.431 ± 0.020	0.358 ± 0.040	0.412 ± 0.032	0.023 ± 0.002
IV-1%	0.9488	0.121 ± 0.034	0.9977	0.500 ± 0.059	0.380 ± 0.109	0.391 ± 0.089	0.025 ± 0.006

Notes: Q – percentage of drug released; k , k_1 and k_2 – rate constants; A and B – the parameters which reflect the portion of the drug released that contributed to the burst and sustained phases, respectively; R^2 – coefficient of determination.

*Sample IV \equiv sample IV-100 \equiv sample IV-3%.

using a modulation of $\pm 0.8^\circ\text{C}$ (amplitude) each 60 s (period) in each step. This allowed residual solvent to be removed from the microparticles and T_g' to be determined. The analyses were done in triplicate.

Thermogravimetric (TG) curves were obtained using a TGA-7 thermogravimetric analyser (Perkin Elmer, Norwalk, CT, USA), using platinum pans with about 5 mg of sample under dynamic nitrogen atmosphere (35 mL/min) and at a heating rate of $10^\circ\text{C}/\text{min}$, from 30°C to 250°C . These analyses enabled the determination of the total amount of the volatile substance (residual solvent). The spectroscopy were done in triplicate.

Fourier transformed infrared analyses

The IR spectra were recorded on a Nicolet 6700 Fourier transformed infrared (FT-IR) instrument (Thermo Fisher Scientific Inc., Waltham, MA, USA) equipped with a fast recovery deuterated triglycine sulphate (DTGS) detector, working under the Omnic software version 4.1. A spectra of $400\text{--}4000\text{ cm}^{-1}$, resolution of 4 cm^{-1} and accumulation of 32 scans were used to obtain good-quality spectra. The KBr disc method was used with approximately 0.5% (w/w) of sample loading.

Fourier transformed Raman spectroscopy

Raman spectra were collected on a Nicolet 6700 FT-IR spectrometer with an NXR FT-Raman module (Thermo Fisher Scientific Inc., Waltham, MA, USA), equipped with a 1064-nm Nd:YVO4 excitation laser, CaF_2 beamsplitter and Ge detector. Data were collected using Omnic software version 4.1. A spectral range of $3700\text{--}400\text{ cm}^{-1}$ was employed with 4 cm^{-1} resolution and accumulation 128.

X-ray powder diffraction analyses

X-ray powder diffraction (XRPD) data were recorded on a Philips X'Pert PRO diffractometer (PAN Analytical, Kassel Waldau, Germany) equipped with an X'Celerator detector ($2.022^\circ 2\theta$) using $\text{Cu-K}\alpha$ radiation at 45 kV and 40 mV. The scan angle range (2θ) was $2\text{--}50^\circ$, the step size (2θ) was 0.017° and the time per step was 50 s. Samples were powdered using mortar and pestle and applied directly into a Phillips' original circular sample holder (16 mm diameter), manually pressed with the sample preparation kit and closed with the bottom plate. Diffractograms were analysed using X'Pert Data Collector software.

Scanning electron microscopy

The morphology of the microspheres was observed by scanning electron microscopy (SEM; JEOL, Type JSM-5800, Tokyo, Japan). Prior to examination, the samples were mounted on a double-sided adhesive and coated

with a thin layer of gold, under vacuum. The scanning electron microscope was operated at an acceleration voltage of 15 kV.

Antimicrobial activity

The antimicrobial activity of drug-loaded microparticles was investigated and compared to the drug and drug-free microparticles activity as control. Microparticles were suspended while the drug was dissolved in degassed pH 5.5 USP acetate buffer (dissolution medium) immediately prior to examination obtaining final drug concentration of $400\text{ }\mu\text{g}/\text{mL}$. Additionally, samples obtained at the end of *in vitro* release testing of the microparticles were subjected to antimicrobial testing.

Antimicrobial activity was tested on *S. aureus* (ATCC 29213; ATCC, American Type Culture Collection). Twofold microdilution assay using Mueller–Hinton broth (Sigma, Munich, Germany) was carried out following CLSI guidelines (National Committee for Clinical Laboratory Standards, 2001). A $1\text{--}2 \times 10^8$ colony-forming unit (cfu)/mL inoculum was prepared and adjusted to a final concentration of $1\text{--}2 \times 10^5$ cfu/mL in broth containing drug, drug-loaded microparticles and drug released from microparticles in twofold dilutions ranging from 0.0625 to $256\text{ }\mu\text{g}/\text{mL}$ on a microtitre plate. Culture of *S. aureus* in the broth was used as positive (growth) control, while broth without *S. aureus* as negative control. The minimal inhibitory concentration (MIC) was recorded as the lowest concentration of mupirocin calcium that inhibited visible bacterial growth after 18 h of incubation at $35 \pm 2^\circ\text{C}$. After incubation of 3, 6 and 18 h, dilutions ($10\text{ }\mu\text{L}$) were subcultured on Mueller–Hinton agar plates and the formation of colonies was observed after 18 h of incubation at $35 \pm 2^\circ\text{C}$. In this experiment, the lowest concentration of mupirocin calcium-containing samples at which *S. aureus* count was reduced by 99% of initial inoculum was recorded as minimal bactericidal concentration (MBC) in relation to the time of incubation. All experiments were done in triplicate.

Statistical analysis

The results are expressed as the mean \pm standard deviation (SD). A one-way analysis of variance was employed in the comparison of the experimental data. *Post-hoc* multiple comparisons were done by Tukey's test for significance at *p*-values less than 0.05 ($p < 0.05$).

Results and discussion

Influence of drug loading on microparticle performance

By altering the initial saturation of feed constituents, different particle solidification patterns and deposition kinetics were expected. Additionally, although rarely

examined for controlled microparticle delivery systems, the higher ratios of drug to polymer were studied. The rationale for such experimental design is based on the assumption that the radial distribution of components within a particle depends on the initial saturation and diffusivity of each solute in a solution intended to be used in spray drying, affecting also particle morphology and density (Bain et al., 1999; Kim et al., 2003; Lechuga-Ballesteros et al., 2008; Wang and Langrish, 2009). During drying, there is a diffusion of solvent towards the surface and solute/s towards the centre because of the concentration gradient caused by the evaporation of solvent from the droplet surface. Transport velocities of different solutes will depend on the concentration gradient, the medium viscosity and the solute diffusivity (Kim et al., 2003; Wang and Langrish, 2009).

Drug loading, morphology and particle size

Yields of powders produced were in the range 53–59%. The microparticles were in the form of a fine white powder. Drug loading for each microparticle composition was in compliance with theoretical values (Table 1). These observations of successful microencapsulation by spray drying from solution (drug and polymer being both dissolved) are already reported in the literature (Pignatello et al., 1997; Wang and Wang, 2002; Rassa et al., 2008). The methodology that uses the solution of polymer and drug provides a homogeneous distribution of solutes in the initially atomised microdroplet. The inherent homogeneity of the starting solution is retained within the drying droplet, resulting in microparticles having drug loading similar to that of the initial solution. However, depending on the rate of the solvent evaporation, the diffusivity of the solutes and potential surface activity, the radial distribution of the drug and polymer may be changed within a particle before complete solidification is reached (Vehring, 2008).

Figure 2 represents the SEM images of all drug-loaded microparticles differing in drug : polymer ratio. Figures 2(a) and 2(e) represent microparticles of the lowest (sample I) and the highest drug loading (sample V), respectively. For both of them, deviation from the spherical shape is easily observed. The morphology of microparticles has been markedly influenced by drug loading; various ratios of drug and polymer influenced deposition kinetics due to different initial saturations resulting in diverse morphologies. In contrast, microparticles having 1:2 (sample II, Figure 2(b)), 1:1 (sample III, Figure 2(c)) and 2:1 (sample IV, Figure 2(d)) drug:polymer ratios (w/w) are mostly spherical with seemingly smooth surfaces absent of visible pores and other major surface discontinuities. No free or incorporated drug crystals were observed on their surface. The surface is generally smooth when polymer precipitates slowly with sufficient time to shrink its size and occurs due to either slow removal of organic solvent or high solubility of solutes in the particular solvent (Bain et al., 1999; Mandal et al., 2001). When higher amounts of either drug or polymer have been used (samples I and V, respectively), higher initial saturations

could have induced an earlier onset of phase transition in the drying droplet, affecting the morphologies of microparticles obtained (Wang and Wang, 2002). The increased polymer content resulted in wrinkled particles, which were probably formed earlier in the drying process with a polymer-enriched soft surface layer (crust) that folded to form the wrinkled particles (Vehring, 2008).

The particle size analysis results suggest that the particles were of similar size with mean spherical diameter ranging between 1.7 and 2.5 μm (Table 1). Small particle sizes could be attributed to the relatively low viscosity of the spraying solution (low concentration of solutes) and high compressed nitrogen flow rate. Additionally, no correlation has been found between drug loading and the particle sizes obtained.

Solid-state characterisation of microparticles

X-ray diffractograms of crystalline and spray dried drug microparticles having different drug:polymer ratios (w/w) (samples I-V) and spray dried polymer are shown in Figure 3. Mupirocin calcium lost its regular ordered lattice structure, becoming amorphous during the spray drying process, with a typical halo baseline observed in the X-ray diffractogram. Amorphous halos are slightly different among particular microparticles due to differences in the weight ratios of the drug and the polymer. All these observations suggest that mupirocin calcium and polymer structure solid dispersion with no measurable crystallisation of the drug. Formation of amorphous structure could be connected to a short precipitation window, which disables the crystallisation process, and the drug remains in a fairly disordered form.

Thermal analyses of such amorphous systems enable the determination of drug and polymer miscibility behaviour using the well-known Gordon-Taylor (GT) equation:

$$T_g = \frac{(w_1 T_{g1} + Kw_2 T_{g2})}{(w_1 + Kw_2)} \quad (1)$$

$$K = \frac{\rho_1 T_{g1}}{\rho_2 T_{g2}} \quad (2)$$

where T_g is the glass transition temperature of a mixture; T_{g_i} , w_i and ρ_i are the glass transition temperature, weight fraction and density of each mixture component (Hancock and Zografi, 1997; Wiranidchabong et al., 2008). This equation predicts the behaviour of a binary mixture based on free volume theory assuming no specific interaction between two components. It is helpful in determining if nonidealities of prepared microsystems exist (e.g. specific drug-polymer interactions, immiscibility) (Hancock and Zografi, 1997).

The thermogram of crystalline drug is characterised by an endothermic peak appearing at the midpoint temperature of 133.9°C and was attributed to the melting point (T_m). Amorphous, spray dried mupirocin calcium has shown a glass transition temperature (T_g) at $59.1 \pm 0.5^\circ\text{C}$ in reverse heat flow curves that enable the detection of the transition being overlapped with the desolvation endotherm in the total heat flow curve. When a heat-cool-

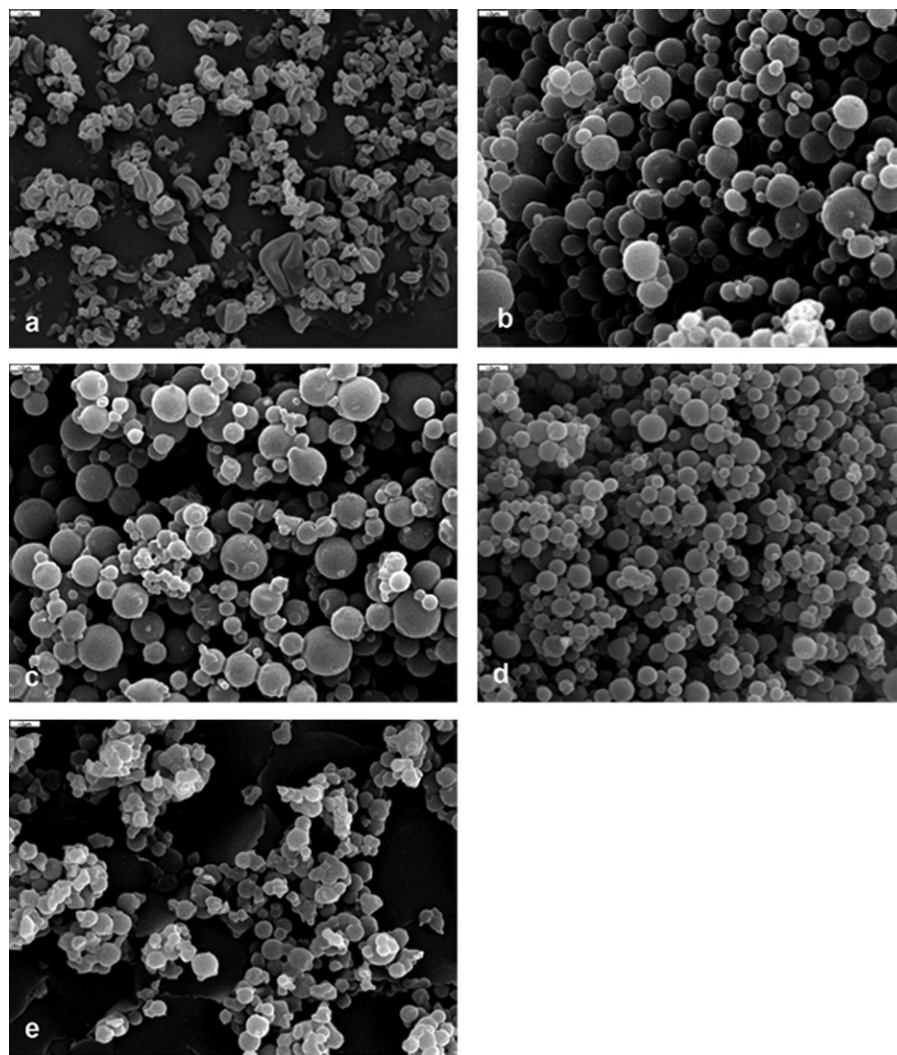


Figure 2. SEM images of the microparticles spray dried at 100°C having different drug : polymer ratios (w/w): (a) sample I; (b) sample II; (c) sample III; (d) sample IV; and (e) sample V.

heat cycle was applied, the glass transition temperature in the second heating run was shifted to $77.8 \pm 0.3^\circ\text{C}$, indicating a plasticising effect of residual methanol ($\sim 1.4\%$) on spray dried mupirocin calcium. The change in specific heat capacity at the glass transition (ΔC_p) for amorphous mupirocin calcium was $0.411 \pm 0.061 \text{ J/g}^\circ\text{C}$. Moreover, spray dried Eudragit[®] RS polymer had a glass transition temperature at $56.3 \pm 0.5^\circ\text{C}$ (Dillen et al., 2006; Sipos et al., 2008) and the change in specific heat capacity at the glass transition (ΔC_p) was $0.156 \pm 0.035 \text{ J/g}^\circ\text{C}$. Residual methanol ($\sim 0.9\%$) had no effect on the glass transition temperature of spray dried polymer, as confirmed by the heat-cool-heat cycle ($T_g' = 56.8 \pm 0.0^\circ\text{C}$).

All microparticle thermograms were characterised by the absence of melting peak at $\sim 133^\circ\text{C}$ indicating that the drug was fully amorphous. These results additionally verify the X-ray findings (Figure 3). A single glass transition temperature has been observed for all microparticles (Table 1), suggesting that drug and polymer structured solid dispersions at the molecular level achieving complete miscibility for all drug : polymer ratios. It is also evident from TGAs that the microparticles contained certain

amounts of residual solvent (Table 1). Samples with higher drug contents (samples IV and V) had somewhat higher amounts of the residual solvent with respect to other microparticles. Based on these data, it was not possible to differentiate if the observed glass transition temperature is a result of microparticle composition or is influenced by residual solvent. The results of glass transition temperature (T_g') obtained using the heat-cool-heat cycle are also shown in Table 1. Residual solvent removal had no effect on the microparticles with the lowest drug content (sample I). The T_g' value ($59.0 \pm 0.4^\circ\text{C}$, Table 1) of these microparticles matched well with the GT predicted value of $\sim 59.5^\circ\text{C}$ (calculated using Equations (1) and (2)), assuming no density differences between drug and polymer. Additionally, T_g' values for samples II-V resulted in glass transition temperatures higher than expected based on the GT equation. However, MDSC analyses of corresponding physical mixtures revealed that the obtained results were not due to the actual increase in T_g' but, rather, as a consequence of phase separation caused by the heat-cool-heat cycle forming a single broad thermal event originating from two consecutive thermal events of

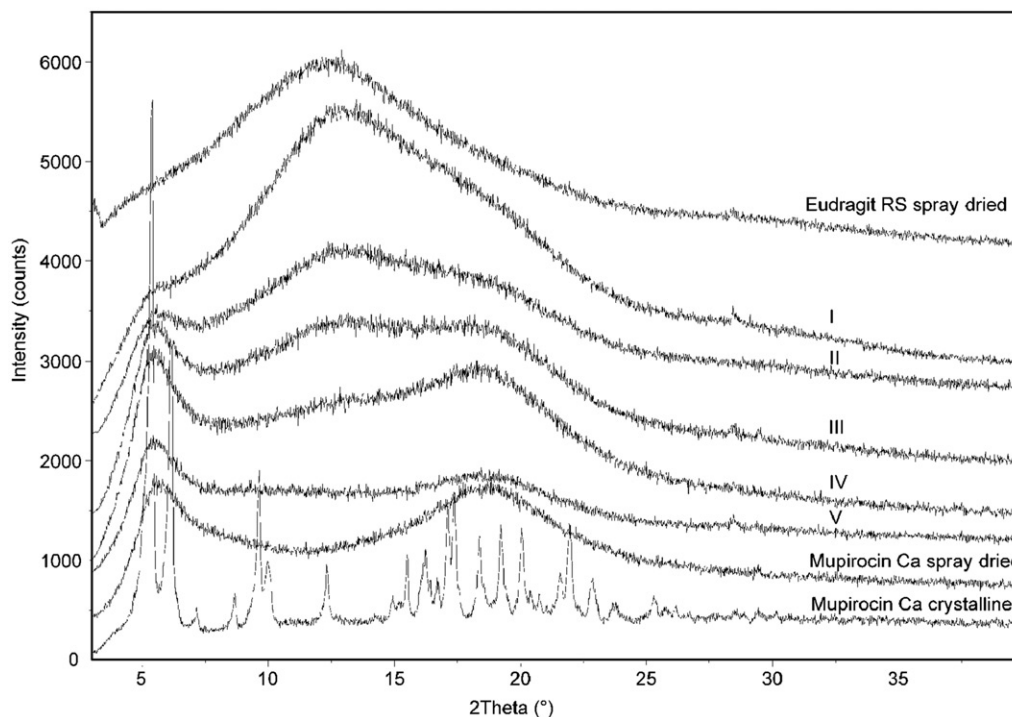


Figure 3. X-ray diffractograms of the crystalline and spray dried mupirocin calcium, microparticles (samples I-V) and spray dried polymer.

the drug and polymer. Therefore, only limited information about solvent influence on microparticles was gained using the heat-cool-heat methodology. This also precluded interpretation of T_g values in terms of possible deviations from GT predictions.

To further understand microparticle fine structure, FT-IR and Raman analyses were conducted. The microparticle spectra were compared to the spectra of amorphous drug and polymer prepared by the same procedure. The FT-IR spectra of microparticles (Figure 4(a)) corresponded to the actual composition of drug and polymer, i.e. generally corresponded to the spectra of its physical mixtures. However, the region of carbonyl stretching, $1700\text{--}1750\text{ cm}^{-1}$, assigned to the ester group for both drug and polymer shows discrepancy between microparticles and the physical mixture in terms of the shape and position of bands. The C=O stretching at 1713 cm^{-1} in the spectra of the amorphous drug was shifted to higher wavenumbers in the spectra of sample IV, seen as the shoulder at 1695 cm^{-1} (Figure 4(b)).

Raman spectra (Figure 5) exhibited even more pronounced bands in the region of carbonyl stretching giving complementary information to the FT-IR spectra. The C=O band stretching in the Raman spectra is observed at 1710.9 cm^{-1} for drug and at 1727.4 cm^{-1} for polymer, while the spectrum of microparticle sample IV (2:1 (w/w) drug:polymer ratio) exhibited a single band for the corresponding carbonyl stretching band at 1722.2 cm^{-1} ; this band shifted to higher wavenumbers with respect to the drug and to lower wavenumbers with respect to the polymer. Moreover, the Raman spectrum of sample III (1:1 (w/w) drug:polymer ratio) exhibited carbonyl stretching at 1714.0 cm^{-1} , which was also shifted to

higher wavenumbers with respect to the same band of the drug. Therefore, the altered molecular surroundings of the drug proved to be present within microparticles and were presumed to be affected by molecular interactions between the drug and the polymer chains. Weaker drug-polymer intermolecular hydrogen bonding, in comparison to drug-drug interactions, were revealed due to the C=O band shift towards higher wavenumbers. These findings provide evidence of the existence of finely dispersed drug and polymer within the microparticles for the examined samples III and IV.

On the other hand, for the case of 5:1 (w/w) drug:polymer ratio (sample V), the C=O stretching band in the FT-IR spectra (Figure 4) was split into two bands, with 1732 and 1714 cm^{-1} positions reflecting the presence of a separated amorphous drug phase. This finding shows that even though a single glass transition event was observed in MDSC, phase separation was detected using FT-IR measurements. This may be partially attributed to the inability of the applied MDSC methodology to separate very close thermal events. Janssens et al. (2008) also reported that a single glass transition event was obtained even though X-ray photoelectron spectroscopy indicated the presence of more than a one phase.

In vitro drug release study

Figure 6 shows the drug release profiles obtained for microparticles containing different drug loadings. Mathematical modelling was used to analyse the drug release profiles (Table 4). The selection of the model was based on the best coefficient of determination and the best graphic adjustment. All microparticles were best fitted by a biexponential model (Table 4).

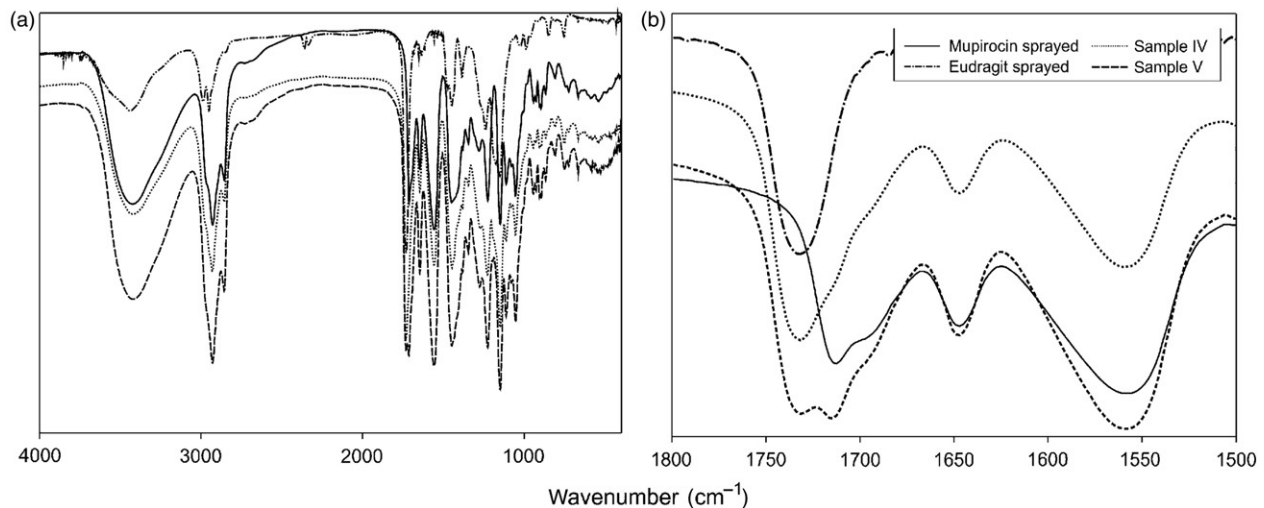


Figure 4. (a) FT-IR spectra of the drug, polymer and microparticles having different drug:polymer ratios (w/w): sample IV (2:1) and sample V (5:1). (b) FT-IR spectra (zoomed region between 1500 and 1800 cm^{-1}) of the drug, polymer and microparticles having different drug:polymer ratios (w/w): sample IV (2:1) and sample V (5:1).

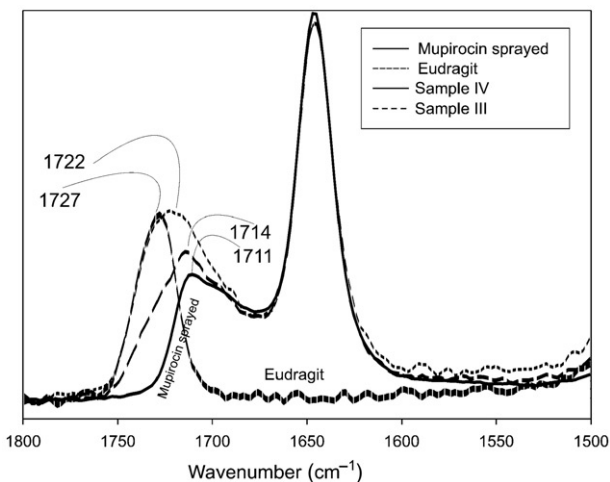


Figure 5. Raman spectra of the drug, polymer and microparticles having different drug:polymer ratios (w/w): sample III (1:1) and sample IV (2:1).

As can be observed, the initial concentration of drug which contributed to the burst release (parameter A) ranged from $\sim 51\%$ ($A = 0.506 \pm 0.036$) for sample IV to $\sim 79\%$ ($A = 0.792 \pm 0.007$) sample V. Additionally, the burst rate constants were higher for microparticles II, III and V, spanning between 0.503 and 0.556 min^{-1} . The burst phase rate constants for the slowest microparticles IV and I were 0.376 ± 0.063 and 0.479 ± 0.044 min^{-1} , respectively.

Surprisingly, the lowest burst release ($\sim 51\%$) was observed for the microparticles containing 2:1 (w/w) drug:polymer ratio (sample IV). Drug release patterns from these microparticles progressed slowly reaching $86.7 \pm 1.5\%$ of the drug released after 3h. Additionally, the sample containing the highest polymer content (sample I) also showed decreased burst release ($\sim 64\%$), with $86.6 \pm 1.7\%$ of the drug being released after 3h. Other microparticles (samples II, III and V) were

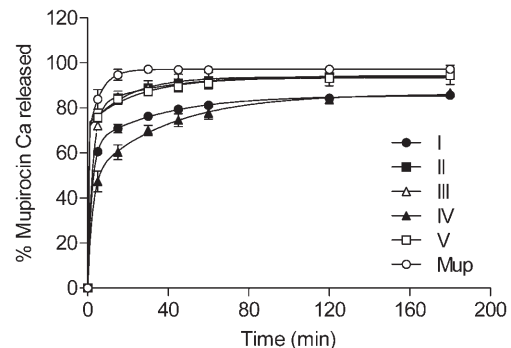


Figure 6. *In vitro* drug release profiles of the microparticles prepared from different drug:polymer ratios (w/w) (samples I-V) in comparison to drug. Data are the mean \pm SD ($n = 3$). In some cases, the error bars are within the size of data point.

characterised by extremely high burst release too deficient to provide adequate controlled release pattern.

The increased polymer weight ratio (sample I) was expected to result in decreased drug release (Al-Zoubi et al., 2008) due to its water-insoluble nature, but these microparticles still presented high burst release ($\sim 64\%$). Solid-state characterisation revealed that the drug was amorphous and fully dispersed within the polymer matrix. Conversion of the drug into its amorphous form promoted drug solubility ($> 95\%$ of drug dissolved within 5 min), which is not favourable for the preparation of a controlled-release system and could have impact on burst release to a certain extent. However, it was assumed that the dissolution medium would not be able to approach drug molecules rapidly if the drug was enveloped or incorporated within a polymer matrix that is insoluble and low permeable. However, this theory was not proven by the results. Possible reason could be found in polymer deposition kinetics. Bain et al. (1999) and Yeo and Park (2004) described that under conditions of rapid

microdroplet desolvation, abrupt polymer precipitation results in low polymer density. Polymer chains do not have enough time for the controlled deposition, and the less dense matrices are formed despite the apparent pore-free nature of all samples examined by SEM. Low polymer density allows dissolution medium to enter and boost drug release. The wrinkled and folded morphology of these microparticles additionally supported the hypothesis that polymer deposition process was rapid and insufficient to make an appropriate matrix.

The microparticles containing a drug:polymer ratio of 2:1 (w/w) (sample IV) created a release pattern that was unexpected. The reduced burst (~51%) and overall drug release profile followed by incomplete drug release from microparticles after 3 h indicated that the polymer matrix formed under examined experimental conditions was superior with regard to the others. These microparticles were amorphous in nature, with no apparent crystallisation. Spectroscopic analyses (FT-IR and FT-Raman) revealed the existence of a molecular solid dispersion of drug and polymer, without the presence of a separate amorphous drug phase. There was no interaction between the drug and polymer that might have decreased drug solubility and interfered with the release process. In addition, the particle size distribution results and SEM images have shown that these microparticles were the smallest in size, contrary to the observed release data. The smooth surfaces and the extremely regular spherical forms of these microparticles indicated that the particles were probably formed slowly and later in drying process (Wang and Wang, 2002). A certain likelihood existed that the solidification process influenced drug release properties also. We assume that lower polymer loading decreased its initial saturation that, in turn, postponed matrix formation in droplet drying and enabled a better arrangement of polymeric chains.

Additional experiments were conducted to test our hypothesis and broaden the understanding of particle formation by varying inlet temperature and feed concentration to alter particle solidification process.

Influence of inlet temperature and feed concentration on microparticle performance

Inlet temperature directly influences evaporation process which determines droplet surface recession rate and strongly affects particle morphology (Vehring et al., 2007). The evaporation of spray dried droplet commences with solvent removal at nearly a constant rate and constant droplet surface temperature, as long as its outer layer is saturated with solvent continuously supplied from the droplet interior. This step is followed by a decline in the removal rate due to increased resistance to mass transfer within the solidifying particle. Consequently, the rate of heat transfer exceeds the rate of mass transfer causing an increase in particle surface (and interior) temperature. When a much higher inlet temperature is used, what results is a rapid formation of the dried outer layer, significantly

reducing period of constant drying rate. This submits the microparticle to the higher surface temperature than when lower inlet temperature is used (Masters, 1985).

The feed concentration, on the other hand, determines the initial saturation of microdroplet constituents, causing an earlier or later solidification onset. The feed concentration is also closely related to microparticle size.

Drug loading, morphology and particle size

Production yield was between 54% and 65% for inlet temperature and feed concentration experiments. Drug loading was consistent with theoretical values for all microparticles (Tables 2 and 3). SEM images (Figure 7) of drug-loaded microparticles prepared with a drug:polymer ratio of 2:1 (w/w) at inlet temperature ranging between 70°C and 110°C have shown essentially identical morphologies, with smooth particles surfaces, no pores or deformations. Temperature variation and consequent change of evaporation rate have not had a crucial impact on the particle outward appearance. The particle size analysis results suggest that particles were of comparable size, with a mean spherical diameter of 1.7–2.5 µm (Table 2).

Microparticles prepared from 1% (w/w) feed solution (sample IV-1%) are highly fused and agglomerated (Figure 8(a)). These agglomerates were mainly formed during drying; microparticles deviated from being spherical in shape probably due to the collision of microdroplets in drying cylinder. It is assumed that fine droplets that were formed after atomisation had very low solid content and low viscosity, resulting in fragile air-solution boundary that allowed particles to deform. Other samples prepared from different feed concentrations ranking from 2% to 5% (w/w) (Figures 8(b)–(d)) showed similar spherical morphology and smooth surfaces. Visually bigger individual particles were formed when more concentrated solutions were spray dried (Elversson et al. 2003; Elversson and Millqvist-Fureby, 2005), although all microparticles were of similar size (Table 3). Increased concentration of solutes in the microdroplets favoured earlier formation of the solid surface (solidification point was reached earlier), which discontinued further droplet surface recession and shrinkage. In addition, the higher solid content increased the viscosity of the feed solution as well (data not shown), which, in turn, resulted in bigger droplets created in the atomisation process and formed the bigger particles.

Solid-state characterisation of microparticles

X-ray diffractograms of microparticles produced at different inlet temperatures and from different feed concentrations confirmed the amorphous nature of the drug without noticeable crystallisation. For the same samples, FT-IR analyses were essentially the same (data not shown).

A trend of decreasing glass transition temperature is evident when inlet temperature is lowered (Table 2). The glass transition temperatures of samples IV-110 and IV-70 significantly differed ($p < 0.05$), while other results do not show statistical differences ($p > 0.05$) among each other (Table 2). It is also apparent that higher solvent

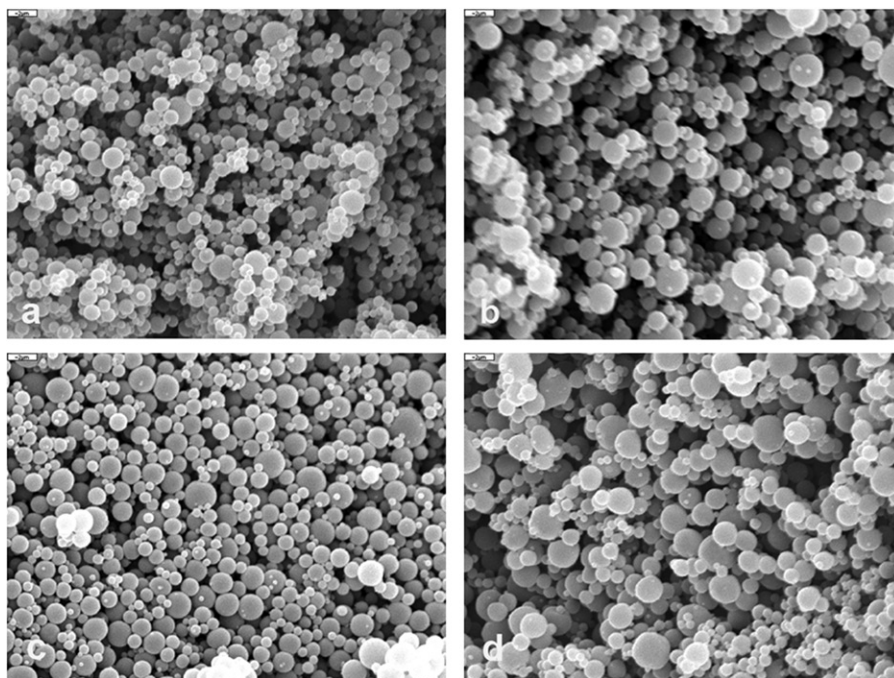


Figure 7. SEM images of microparticles having drug:polymer ratio 2:1 (w/w) prepared from 3% feed solution at different temperatures: (a) IV-110; (b) IV-90; (c) IV-80; and (d) IV-70.

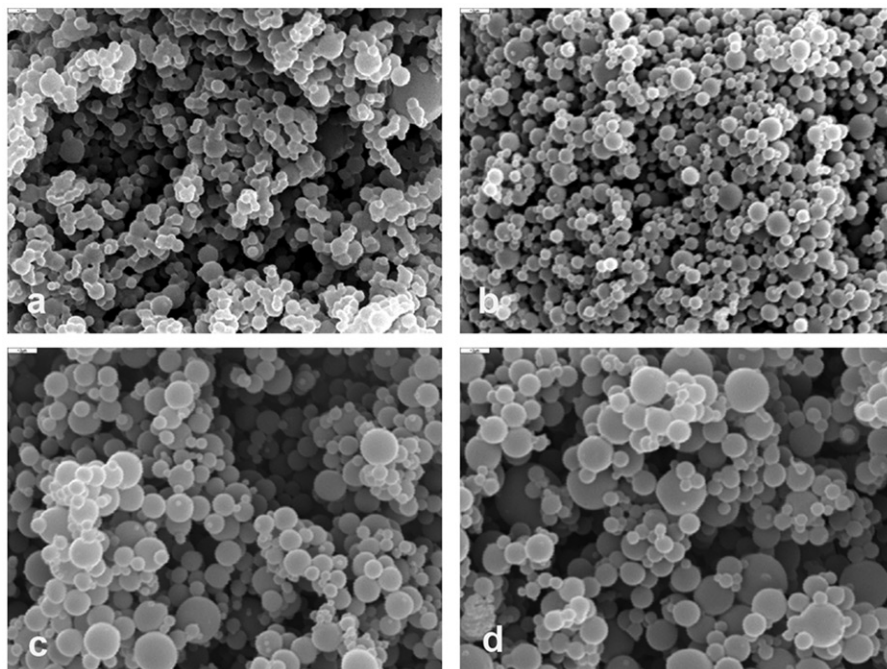


Figure 8. SEM images of microparticles having drug:polymer ratio 2:1 (w/w) spray dried at 100°C from different feed solutions: (a) sample IV-1%; (b) sample IV-2%; (c) sample IV-4%; and (d) sample IV-5%.

residues were associated with lower T_g values, suggesting that residual solvent could provide a plasticising effect to microparticles (Table 2). For the microparticles obtained by spray drying of different feed solutions at 100°C, there was no significant difference ($p > 0.05$) between the glass transition temperatures (Table 3). Solvent residues were present at the highest level ($\sim 1.6\%$, Table 3) in the sample prepared from the most concentrated feed

solution (IV-5%). Once again, the highest residual solvent value was related to the lowest glass transition temperature ($63.1 \pm 1.5^\circ\text{C}$) obtained for the sample IV-5% (Table 3).

In vitro drug release study

Regarding the modelling of the drug release profiles, the best fit was the biexponential equation for all

microparticles (Table 4). The burst drug release decreased significantly ($p < 0.05$) from $\sim 51\%$ ($A = 0.506 \pm 0.036$, sample IV-100) to $\sim 32\%$ ($A = 0.321 \pm 0.029$, sample IV-110) when the inlet temperature was raised from 100°C to 110°C (Figure 9). It is also evident that at lower inlet temperatures, specifically 90°C , 80°C and 70°C , burst release increased up to $\sim 76\%$ ($A = 0.761 \pm 0.005$), $\sim 79\%$ (0.786 ± 0.010) and $\sim 72\%$ ($A = 0.724 \pm 0.007$), respectively. The burst rate constant for sample IV-110 reached the lowest value of $0.346 \pm 0.061 \text{ min}^{-1}$. However, a significant difference ($p > 0.05$) was not confirmed between microparticles prepared at 100°C and 110°C when burst rate constants were compared.

Results suggest that the inlet temperature affected burst release and the overall release profile; higher temperature favoured lower drug release. As previously depicted, a certain trend in the thermal properties was noticed and requires further consideration. The effect of temperature on a microparticle during its lifetime in a drying chamber has been thoroughly considered. The higher inlet temperature (much higher than the boiling point of solvent) induced more rapid solvent evaporation that enabled the onset of rapid solidification. The droplet lifetime was dramatically reduced, and, under an equal aspirator setting, microparticles prepared at a higher temperature existed for a longer period of time in a more heated environment inside the drying chamber. Temperature affected the physical properties of the solidifying polymer matrix, enhancing molecular mobility when increased over the glass transition temperature. For amorphous polymers, greater chain mobility enables relaxation processes to happen, resulting in reduced free volume and increased density (Craig et al., 1999). It is assumed that such thermal treatment may improve matrix density by allowing necessary configurational changes to occur (Azarmi et al., 2002). Additionally, lower solvent residues observed in these microparticles (sample IV-100 and IV-110) reduced the plasticising effect of solvent. Such matrices are characterised by increased intermolecular forces along the polymer chains, which could create a denser polymer matrix. All these events could limit dissolution medium penetration and slow down drug release. A similar observation of decreased drug release for biodegradable microparticles at higher inlet temperatures due to increased particle density has already been reported by Fu et al. (2001). In contrast, microparticles spray dried at inlet temperatures below 100°C (samples IV-90, IV-80 and IV-70) have not resulted in the rubbery state being glassy earlier in the drying process (see outlet temperatures, Table 2), which prevents molecular rearrangement and densification to occur even though evaporation rate was slower. This hypothesis is in agreement with the trend observed for the glass transition temperatures of corresponding microparticles, even though the differences between results are not statistically significant. Drug diffusion pathways in microparticle systems are extremely shortened in comparison to macroscopic controlled-delivery systems. Any deviation in matrix formation could be easily observed in prominent burst release; therefore, even small changes of

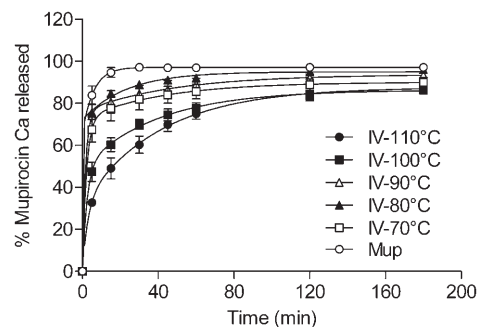


Figure 9. *In vitro* drug release profiles of microparticles having drug: polymer ratio 2:1 (w/w) prepared from 3% feed solution at different temperatures (samples IV-110, IV-100, IV-90, IV-80 and IV-70) in comparison to drug. Data are the mean \pm SD ($n = 3$). In some cases, the error bars are within the size of data point.

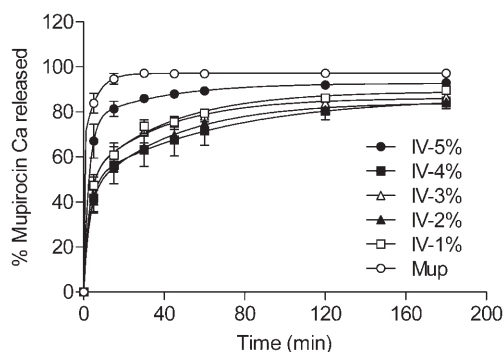


Figure 10. *In vitro* drug release profiles of microparticles having drug: polymer ratio 2:1 (w/w) spray dried at 100°C from different feed solutions (samples IV-1%, IV-2%, IV-3%, IV-4% and IV-5%) in comparison to drug. Data are the mean \pm SD ($n = 3$). In some cases, the error bars are within the size of data point.

glass transition temperature associated with the particle density (Bouissou et al., 2006) should be carefully evaluated.

In vitro drug release profiles obtained for microparticles spray dried from different feed solutions are shown in Figure 10. Again, the best fitting for all microparticles was achieved with the biexponential model (Table 4). Initial burst release obtained for the microparticles prepared from 5% (w/w) (sample IV-5%) solution approached 76% ($A = 0.759 \pm 0.010$) and was significantly higher ($p < 0.05$) in regard to all the other samples that remained between 43% and 50%. The burst rate constant ($k_1 = 0.424 \pm 0.017 \text{ min}^{-1}$) of the microparticles prepared from 5% (w/w) (sample IV-5%) solution was higher in regard to the burst rate constants obtained for all other samples that remained between 0.315 and 0.380 min^{-1} , but a significant difference has not been confirmed. Drug release profiles obtained for IV-1%–IV-5% microparticles (Figure 10) revealed that drug release changes nonlinearly with the increase in feed concentration. It was unaffected when the feed concentration increased from 1% to 4% (w/w), but it changed when concentration approached 5% (w/w).

Table 5. MBCs of mupirocin calcium and mupirocin calcium-loaded microparticles tested on *S. aureus* (ATCC 29213) ($n=3$).

Sample	MBC ($\mu\text{g/mL}$) 3 h	MBC ($\mu\text{g/mL}$) 6 h	MBC ($\mu\text{g/mL}$) 18 h
Mupirocin calcium	128	32	16
IV	128-256	64-128	16
IV-110	128-256	64-128	16
IV (drug released from microparticles)	128	32	16
IV-110 (drug released from microparticles)	128	32	16

Variation of feed concentration affects the timing of particle formation under equal processing conditions (Elversson and Millqvist-Fureby, 2005). Apparently, the solidification takes place earlier in the drying process when higher feed concentration is used (Lechuga-Ballesteros et al., 2008). Early onset of the particle formation due to higher initial saturation leaves less time for drying droplet to shrink its size and increase particle density. The microparticles are practically “frozen”, leaving polymer chains loosely packed (Yeo and Park, 2004). It appears that under examined spray drying condition, 5% (w/w) feed concentration had too high of an initial saturation inducing early solidification too deficient to obtain controlled release pattern. Additionally, early formation of outer layer entrapped more solvent within IV-5% sample (1.6%, Table 3). The presence of the solvent could plasticise polymer matrix contributing to the observed burst release. Nevertheless, morphological characteristics are frequently reported to be directly related to drug release profiles, but visually similar spherical microparticles exhibited significantly different drug release profiles in this study.

In summary, the inlet temperature and feed concentration experiments demonstrated that the particle formation process could be responsible for controlling drug release pattern initially observed for the samples containing drug:polymer ratio 2:1 (w/w) rather than formulation composition itself. The best control over mupirocin calcium release, with significantly decreased drug release, was obtained for microparticles having a 2:1 (w/w) drug:polymer ratio prepared at a 110°C inlet temperature from 3% (w/w) feed solution using a laboratory scale equipment. These microparticles deserve further evaluation as promising candidates for the development of topical controlled-release systems.

Antimicrobial activity

Antimicrobial activity of drug-loaded microparticles was compared with drug-free microparticles, drug released from the microparticles and drug alone. Microparticles IV and IV-110 were chosen for antimicrobial activity testing due to the most favourable drug release achieved. MIC was 0.125 $\mu\text{g/mL}$ for each tested sample upon 18 h of incubation. As expected, drug-free microparticles exhibited no antimicrobial activity. Moreover, MBCs were concentration- and time-dependent for all samples showing slow bactericidal activity (Table 5). MIC value was significantly lower than concentration needed to kill 99% of initially

inoculated bacteria after 18 h of incubation, which is in accordance with previously studied mupirocin bactericidal activity (Sutherland et al., 1985). After 3 and 6 h of incubation, MBCs were twofold higher for drug-loaded microparticles than for mupirocin calcium released from the microparticles or mupirocin calcium itself. Higher MBCs values originate from the slower drug release obtained from the polymer matrix that is in agreement with desired performance of delivery systems. However, potential usage of such systems in therapy requires adjustment of initial drug concentration needed to maintain appropriate drug levels on skin during prolonged time. After 18 h of incubation, MBCs were similar for all drug-containing samples. These results confirm that encapsulation of mupirocin calcium does not compromise its antibacterial activity.

Conclusion

The preparation of microparticles for controlled drug release via spray drying is a complex task accompanied with challenges to overcome burst release. This research has shown that mupirocin calcium-loaded microparticles intended for controlled drug release could be obtained even with a high loading (~66% (w/w)) of readily soluble drug when appropriate spray drying conditions are achieved and polymer deposition kinetics allows appropriate matrices to be formed. Also, antimicrobial activity testing confirms that encapsulated drug preserves its antibacterial effectiveness. Drug loading solely is not a sufficient and reliable predictor of drug release pattern and should be evaluated in conjunction with corresponding processing parameters. Microparticles intended for controlled drug delivery necessitate the formation of well-formed (denser) matrices that could be tailored via appropriate spray drying processing, given that even small variations in the process may profoundly change delivery system performance. Initial saturation of drug and polymer as well as inlet temperature, were recognised as efficient tools to modulate the formation of proper polymer matrices.

Acknowledgements

The authors thank PLIVA Croatia Ltd for financial support of this research. The authors also thank Mr Marjan Tudja for his kind support in SEM imaging, Mrs Nada Hulita-Košutić and Mr Tomislav Biljan for their help in XRPD analyses.

Declaration of interest

The authors report no conflicts of interest. The authors alone are responsible for the content and writing of this article.

References

- Al-Zoubi N, Alkhatib HS, Bustanji Y, Aiedeh K, Malamataris S. Sustained-release of buspirone HCl by co spray-drying with aqueous polymeric dispersions. *Eur J Pharm Biopharm*, 2008;69:735–42.
- Amrutiya N, Bajaj A, Madan M. Development of microsponges for topical delivery of mupirocin. *AAPS PharmSciTech*, 2009;10:402–9.
- Azarmi S, Farid J, Nokhodchi A, Bahari-Saravi SM, Valizadeh H. Thermal treating as a tool for sustained release of indomethacin from Eudragit RS and RL matrices. *Int J Pharm*, 2002;246:171–7.
- Bain DF, Munday DL, Smith A. Solvent influence on spray-dried biodegradable microspheres. *J Microencapsul*, 1999;16:453–74.
- Beck RC, Pohlmann AR, Hoffmeister C, Gallas MR, Collnot E, Schaefer UF, Guterres SS, Lehr CM. Dexamethasone-loaded nanoparticle-coated microparticles: Correlation between in vitro drug release and drug transport across Caco-2 cell monolayers. *Eur J Pharm Biopharm*, 2007;67:18–30.
- Bouissou C, Rouse JJ, Price R, van der Walle CF. The influence of surfactant on PLGA microsphere glass transition and water sorption: Remodeling the surface morphology to attenuate the burst release. *Pharm Res*, 2006;3:1295–305.
- Chen R, Okamoto H, Danjo K. Preparation of functional composite particles of salbutamol sulfate using a 4-fluid nozzle spray-drying technique. *Chem Pharm Bull (Tokyo)*, 2008;56:254–9.
- Cortesi R, Ajanji SC, Sivieri E, Manservigi M, Fundueanu G, Menegatti E, Esposito E. Eudragit microparticles as a possible tool for ophthalmic administration of acyclovir. *J Microencapsul*, 2007;24:445–56.
- Craig DQ, Royall PG, Kett VL, Hopton ML. The relevance of the amorphous state to pharmaceutical dosage forms: Glassy drugs and freeze dried systems. *Int J Pharm*, 1999;179:179–207.
- Dillen K, Vandervoort J, van den Mooter G, Ludwig A. Evaluation of ciprofloxacin-loaded Eudragit RS100 or RL100/PLGA nanoparticles. *Int J Pharm*, 2006;314:72–82.
- Elversson J, Millqvist-Fureby A. Particle size and density in spray drying-effects of carbohydrate properties. *J Pharm Sci*, 2005;94:2049–60.
- Elversson J, Millqvist-Fureby A, Alderborn G, Elofsson U. Droplet and particle size relationship and shell thickness of inhalable lactose particles during spray drying. *J Pharm Sci*, 2003;92:900–10.
- Embil K, Nacht S. The Microsponge Delivery System (MDS): A topical delivery system with reduced irritancy incorporating multiple triggering mechanisms for the release of actives. *J Microencapsul*, 1996;13:575–88.
- Esposito E, Roncarati R, Cortesi R, Cervellati F, Nastruzzi C. Production of Eudragit microparticles by spray-drying technique: Influence of experimental parameters on morphological and dimensional characteristics. *Pharm Dev Technol*, 2000;5:267–78.
- Fu YJ, Mi FL, Wong TB, Shyu SS. Characteristic and controlled release of anticancer drug loaded poly(D,L-lactide) microparticles prepared by spray drying technique. *J Microencapsul*, 2001;18:733–47.
- Hadinoto K, Phanapavudhikul P, Kewu Z, Tan RB. Dry powder aerosol delivery of large hollow nanoparticulate aggregates as prospective carriers of nanoparticulate drugs: Effects of phospholipids. *Int J Pharm*, 2007;333:187–98.
- Hancock BC, Zografi G. Characteristics and significance of the amorphous state in pharmaceutical systems. *J Pharm Sci*, 1997;86:1–12.
- Janssens S, de Armas HN, Roberts CJ, van den Mooter G. Characterization of ternary solid dispersions of itraconazole, PEG 6000, and HPMC 2910 E5. *J Pharm Sci*, 2008;97:2110–20.
- Kawakami K, Sumitani C, Yoshihashi Y, Yonemochi E, Terada K. Investigation of the dynamic process during spray-drying to improve aerodynamic performance of inhalation particles. *Int J Pharm*, 2010;390:250–9.
- Kim EH-J, Chen XD, Pearce D. On the mechanisms of surface formation and the surface compositions of industrial milk powders. *Drying Technol*, 2003;21:265–78.
- Kristmundsdóttir T, Gudmundsson ÓS, Ingvarsdóttir K. Release of diltiazem from Eudragit microparticles prepared by spray-drying. *Int J Pharm*, 1996;137:159–65.
- Lechuga-Ballesteros D, Charan C, Stults CL, Stevenson CL, Miller DP, Vehring R, Tep V, Kuo MC. Trileucine improves aerosol performance and stability of spray-dried powders for inhalation. *J Pharm Sci*, 2008;97:287–302.
- Lionzo MI, Re MI, Guterres SS, Pohlmann AR. Microparticles prepared with poly(hydroxybutyrate-co-hydroxyvalerate) and poly(epsilon-caprolactone) blends to control the release of a drug model. *J Microencapsul*, 2007;24:175–86.
- Mandal TK, Bostanian LA, Graves RA, Chapman SR, Idodo TU. Porous biodegradable microparticles for delivery of pentamidine. *Eur J Pharm Biopharm*, 2001;52:91–6.
- Masters K, 1985. *Spray drying handbook*. New York, USA: Halsted Press.
- National Committee for Clinical Laboratory Standards. 2001. *Methods for dilution antimicrobial susceptibility tests for bacteria that grow aerobically: Approved standard. M7-A5*. Wayne, PA, NCCLS.
- Pignatello R, Vandelli MA, Giunchedi P, Puglisi G. Properties of tolmetin-loaded Eudragit RL100 and Eudragit RS 100 microparticles prepared by different techniques. *STP Pharm Sci*, 1997;7:148–57.
- Rassu G, Gavini E, Spada G, Giunchedi P, Marceddu S. Ketoprofen spray-dried microspheres based on Eudragit RS and RL: Study of the manufacturing parameters. *Drug Dev Ind Pharm*, 2008;34:1178–87.
- Rattes ALR, Oliveira WP. Spray drying conditions and encapsulating composition effects on formation and properties of sodium diclofenac microparticles. *Powder Technol*, 2007;171:7–14.
- Sipos P, Szabó A, Eő s I, Szabó-Révész P. A DSC and Raman spectroscopic study of microspheres prepared with polar cosolvents by different techniques. *J Therm Anal Calorim*, 2008;94:109–18.
- Sutherland R, Boon RJ, Griffin KE, Masters PJ, Slocombe B, White AR. Antibacterial activity of mupirocin (pseudomonic acid), a new antibiotic for topical use. *Antimicrob Agents Chemother*, 1985;27:495–8.
- Vehring R. *Pharmaceutical particle engineering via spray drying*. *Pharm Res*, 2008;25:999–1022.
- Vehring R, Foss WR, Lechuga-Ballesteros D. Particle formation in spray drying. *J Aerosol Sci*, 2007;38:728–46.
- Wang S, Langrish T. A review of process simulations and the use of additives in spray drying. *Food Res Int*, 2009;42:13–25.
- Wang FJ, Wang CH. Sustained release of etanidazole from spray dried microspheres prepared by non-halogenated solvents. *J Controlled Release*, 2002;81:263–80.
- Ward A, Campoli-Richards DM. Mupirocin. A review of its antibacterial activity, pharmacokinetic properties and therapeutic use. *Drugs*, 1986;32:425–44.
- Wiranidchapong C, Tucker IG, Rades T, Kulvanich P. Miscibility and interactions between 17 β -estradiol and Eudragit[®] RS in solid dispersion. *J Pharm Sci*, 2008;97:4879–88.
- Yeo Y, Park K. Control of encapsulation efficiency and initial burst in polymeric microparticle systems. *Arch Pharm Res*, 2004;27:1–12.